

Article

Alginate-Chitosan Microgel Particles, Water–Oil Interfacial Layers, and Emulsion Stabilization

Aggelos Charisis  and Eleni P. Kalogianni * 

Department of Food Science and Technology, International Hellenic University, Alexander Campus, 57400 Thessaloniki, Greece; agcharisis@food.ihu.gr

* Correspondence: elekalo@ihu.gr

Abstract: In this work, alginate-chitosan microgel particles were formed at different pH levels with the aim of using them as viscoelastic interfacial layers, which confer emulsion stability to food systems. The particles' size and structural characteristics were determined using laser diffraction, confocal laser microscopy (CLSM), and time-domain nuclear magnetic resonance (TD-NMR). The pH affected the microgel characteristics, with larger particles formed at lower pH levels. T_2 relaxation measurements with TD-NMR did not reveal differences in the mobility within the particles for the different pH levels, which could have been related to the more or less swollen structure. The rate of adsorption of the particles at the sunflower oil–water interface differed between particles formed at different pH levels, but the equilibrium interfacial tension of all systems was similar. Higher interfacial dilatational viscoelasticity was obtained for the systems at lower pH (3, 4, 5), with G' reaching 13.6 mN/m (0.1 Hz) at pH 3. The interfacial rheological regime transitioned from a linear elastic regime at lower pH to a linear but more viscoelastic one at higher pH. The thicker, highly elastic interfacial layer at low pH, in combination with the higher charges expected at lower pH, was related to its performance during emulsification and the performance of the emulsion during storage. As revealed by laser diffraction and CLSM, the droplet sizes of emulsions formed at pH 6 and 7 were significantly larger and increased in size during 1 week of storage. CLSM examination of the emulsions revealed bridging flocculation with the higher pH. Nevertheless, all emulsions formed with microgel systems presented macroscopic volumetric stability for periods exceeding 1 week at 25 °C. A potential application of the present systems could be in the formation of stable, low-fat dressings without the addition of any emulsifier, allowing, at the same time, the release of the bioactive compounds for which such particles are known.

Keywords: biopolymer microgels; interfacial tension; interfacial rheology; particle-stabilized emulsions



Citation: Charisis, A.; Kalogianni, E.P. Alginate-Chitosan Microgel Particles, Water–Oil Interfacial Layers, and Emulsion Stabilization. *Colloids Interfaces* **2023**, *7*, 48. <https://doi.org/10.3390/colloids7020048>

Academic Editor: Georgi G. Gochev

Received: 29 May 2023

Revised: 10 June 2023

Accepted: 13 June 2023

Published: 15 June 2023



Copyright: © 2023 by the authors. Licensee MDPI, Basel, Switzerland. This article is an open access article distributed under the terms and conditions of the Creative Commons Attribution (CC BY) license (<https://creativecommons.org/licenses/by/4.0/>).

1. Introduction

Microgels exhibit a variety of characteristics attributed to their binary nature, such as thermal and pH sensitivity, reversible swelling, deformability, and interfacial activity [1–4]. For instance, the temperature, pH, and ionic strength in the external environment can stimulate microgels to swell in the solvent to varying degrees [5–7]. It has been suggested that microgelation can impart emulsifying abilities even to surface-inactive polysaccharides [8,9]. Soft microgels can easily deform and partially interconnect at the interface, which can change the surface coverage and improve the viscoelastic response of the interface, improving emulsion stability [6,10–14]. During recent years, microgels based on edible biopolymers have attracted attention as stabilizing agents in foams and emulsions [15].

The sensitivity of microgels to environmental factors has a significant effect on their behavior at the interface and, thus, on the stability of emulsions stabilized with microgels. Furthermore, reactivity adds functions to microgel-stabilized emulsions, and droplets can be ruptured via external parameters if necessary, which broadens the potential applications for the stimulus-dependent controlled release of bioactive

substances [4,16,17]. Food-grade microgels are composed of supramolecular assemblies of biocompatible and biodegradable biopolymer molecules, such as proteins, polysaccharides, and their complexes [8,18]. Successful synthesis of food microgels can be achieved using various techniques [2,15,19–27]. In the top-down approach, macrogels are broken down into smaller fragments. Gels fracture when the stresses transferred from the surrounding medium exceed the material's cohesive forces [28]. Large amounts of energy must be expended to obtain micro- or submicron-sized gel particles [29]. Mechanical breakage of a bulk hydrogel in the presence of excess solvent is a frequently used approach for the formation of proteinaceous microgels and a promising scalable method to produce microgel particles in the food industry [30–34]. Nevertheless, this “top-down” approach has rarely been used for the preparation of polysaccharide microgels.

Alginate is a commonly used polysaccharide consisting of b-D-mannuronate and a-L-guluronate monomers. In the presence of divalent cations (e.g., calcium ions), the cations bind to the carboxyl groups of the guluronate monomers and form a gel network. Early studies on alginate beads (i.e., millimeter-sized particles) using Ca^{2+} as gelling agent showed pH responsiveness, with the particles swelling at neutral pH and above and keeping their size unchanged at acidic pH [35,36]. Retaining integrity at acidic pH is important for food applications since foods present acidic pH.

Chitosan is a product of chitin deacetylation [37,38]. The degree of deacetylation affects the hydrophilic/hydrophobic character of the molecule, which, in turn, affects chitosan's interfacial and emulsification properties [39]. It has been suggested that chitosan forms polyelectrolytic brushes at the water–oil interface and that emulsion stability is conferred by a both steric and electrostatic barrier [40]. Chitosan is pH-sensitive since the pH affects the degree of protonation of the amino groups present in the molecule [41]. Polycations, such as chitosan, can adsorb on the surface of calcium alginate gels [42]. Strong ionic interactions have been observed between the carboxyl residues of alginate and the amino terminals of polycations [43]. Alginate gel's porosity is reduced by the polycation–alginate complex layer, which, in turn, acts as a further barrier to molecule transport in and out of the gel particles [44,45]. This made possible the formation of millimeter-sized alginate-chitosan particles for drug release over 20 years ago [46–48]. Later on, micro- and nanosized alginate-chitosan particles were produced [49–52]. These particles have shown very good stability and the controlled release properties of active substances in acidic media, as verified by *in vitro* gastrointestinal tract experiments [53]. The change in the size from mm to μm and nm can further expand the applications of these particles.

Studies on the formation and utilization of chitosan and alginate matrices with a core–shell structure have received particular attention. In this regard, Ribeiro et al. [47] developed chitosan-coated alginate microspheres with a lipophilic marker utilizing the emulsification/internal gelation approach in order to potentially use them as an oral controlled-release system. A similar approach was applied by You et al. [50] to create chitosan-alginate core–shell nanoparticles for effective gene transfection. Alginate-chitosan core–shell microcapsules were developed by Taqieddin and Amiji [48] as a biocompatible scaffold for enzyme immobilization. Zhang et al. [51] used membrane emulsification combined with a two-step solidification process to produce alginate-chitosan microspheres with a narrow size distribution. Conti et al. [52] developed alginate/chitosan microspheres using a one-step complex coacervation method to enhance the delivery process for anticaries agents. For the purpose of creating magnetic chitosan-alginate core–shell beads for oral delivery of small molecules, Seth et al. [54] used a common extrusion crosslinking technique. Qin et al. [55] developed stimuli-responsive chitosan-alginate core–shell beads by making use of a one-step dripping technique.

In recent decades, rigid, solid particle-stabilized emulsions have gained significant popularity. Numerous articles have investigated the theories of Pickering stabilization, taking into account the colloidal properties, adsorption behaviors, arrangement on the interface, and interfacial rheological properties of the particles and their correlation with the

particles' emulsifying behavior and emulsion stability [56–58]. Although nondeformable solid particles continue to reign as the most preferred emulsion stabilizers, there has been increasing interest in deformable particles, such as microgels. The stabilization of emulsions with microgels, for instance, shares some similarities with the stabilization achieved with rigid particles, but the underlying mechanisms appear to differ significantly from those observed in Pickering emulsions, and a precise understanding of them remains limited [59].

Given the current knowledge of chitosan-coated alginate microgel formation [49,60–62] and the more hydrophobic nature of chitosan compared to other polysaccharides, chitosan-coated alginate microparticles could be used to form and stabilize emulsions. Emulsion stabilization could then be combined with their encapsulation properties, which could be useful for protection or controlled release of useful active substances [63]. To the best of the authors' knowledge, the only authors who have investigated the ability of chitosan-coated alginate microgels to adsorb on interfaces and form emulsions are Nan et al. [64], who demonstrated the adsorption of these particles on oil–water interfaces; some of the examined systems presented emulsion stability for an hour.

The present work aimed to further investigate chitosan-coated alginate microgels and their ability to adsorb at interfaces and form emulsions. To this end, alginate particles were formed using the top-down approach and coated with chitosan. Microgels were formed at different pH levels; namely, 3, 4, 5, 6, and 7. The particle sizes of the microgels were determined using laser diffraction and the microgel structural characteristics were investigated using confocal laser microscopy (CLSM) and time-domain nuclear magnetic resonance (TD-NMR). The dynamic interfacial tension at the oil–microgel aqueous suspension interface and the dilatational interfacial rheology of the systems at equilibrium were analyzed. Finally, the microgel suspensions were used to prepare sunflower-oil-in-water emulsions without the addition of any other emulsifying or stabilizing agent. The size distributions of the oil-in-water emulsions were determined via laser diffraction and the emulsion microstructures were observed via CLSM. Emulsion stability was determined via droplet size distribution and volumetric phase separation measurements.

2. Materials and Methods

2.1. Materials

Alginate sodium powder with a molecular weight range of 450–550 kDa, chitosan with a deacetylation degree of 90% and molecular weight of 50 kDa, fluorescein isothiocyanate (FITC), Nile red, and calcium chloride dehydrate were all purchased from Sigma Aldrich (St. Louis, MO, USA). Hydrochloric acid and sodium hydroxide were purchased from CHEM-LAB NV (Zedelgem, Belgium). Sunflower oil, which contains saturated fatty acids (11%), monounsaturated acids (C18:1) (35%), and polyunsaturated acids (C18:2) (54%), was obtained from a local market. High-purity water with a resistivity of 18 M Ω .cm at 25 °C was obtained using a Millipore Milli Q Plus/Purelabtex (EIGA Process Water, Marlow, UK) water purification system.

2.2. Preparation of Chitosan-Coated Alginate Microgels

2.2.1. Alginate Microgel Preparation

Sodium alginate powder (1%) was dissolved in deionized water (pH 7 without further adjustment) to form an alginate stock solution. Calcium chloride dihydrate was dissolved in water to achieve a calcium ion concentration of 50 mM. The two solutions containing the sodium alginate and calcium ions were mixed in a 50:50 alginate: Ca²⁺ solution volume ratio and mixed under high shear at 20,000 rpm with an IKA T25 Ultra TURRAX Ultra-homogenizer (IKA®-Werke GmbH & Co. KG, Staufen, Germany) for 2 min. After particle formation, high-speed centrifugation was performed under ambient conditions at 10,000 \times g for 20 min to remove the excess solvent. After centrifugation, washing was performed three times with deionized water to remove the non-crosslinked alginate. After centrifugation performed in triplicate, the alginate particles were separated.

2.2.2. Chitosan Coating

Alginate particles were redispersed in 1 wt% chitosan solution in acetic acid (pH 3) and stirred for 1 h. The microgels were centrifuged, washed with 2% acetic acid solution to remove the excess chitosan, and separated by centrifugation. The chitosan-coated alginate microgels were redispersed in aqueous solutions of pH 3, 4, 5, 6, and 7 and sonicated in an ultrasonic homogenizer (Hielscher UP-100 H, Teltow, Germany; power of 200 Hz and amplitude of 100%) for 5 min. The water–oil interfacial tension of the centrifuged water phase after the above procedure was much higher than that of the alginate or the chitosan solution.

2.3. Particle Sizing of Microgels

The size distribution of the microgel particles was measured using a laser diffraction instrument (Malvern Mastersizer 2000, Malvern, Worcestershire, UK), with the sample fed into the instrument via a Hydro MU liquid sampler (Malvern Instrument, Malvern, Worcestershire, UK). The refractive index of the microgels' dispersed phase was set to 1.50, while the refractive index of the continuous phase was set to 1.33. For the particles, an absorbance value of 0.1 was selected. The particle size distribution was calculated using the Mie equations and angular scattering data. Prior to measurement, the samples were diluted with an appropriate buffer to achieve a laser obscuration between 7% and 10% to reduce the effects of multiple scattering. The buffer was chosen to match the pH of the microgel solution.

2.4. ^1H Relaxometry

^1H relaxometry was performed using a Minispec mq20 (Bruker Corp., Billerica, MA, USA) with a magnetic field strength of 0.47T (proton resonance frequency of 20 MHz). For the relaxometry measurement, 2 mL portions of the prepared microgel suspensions were added into the NMR tubes, and the tubes were placed in the TD-NMR sample compartment. T_2 relaxation decay curves were monitored using the standard Carr–Purcell–Meiboom–Gill (CPMG) pulse sequence. The CPMG decay sequence consisted of 10,000 echoes, which was at least $5\times$ the longest T_2 with an echo time of 1 ms. Experiments were averaged over 16 scans with a repetition time of 30 s. T_2 spectra of relative intensity as a function of T_2 were determined via a numerical inverse Laplace transformation of the data using the software CONTIN (version 2DP) [65]. The regularization parameter in CONTIN was set to a uniform, conservative value for all spectra to ensure the comparability of the results. The signal-to-noise ratio was $\text{SNR} = 400$ and comparable for all measurements. The T_2 spectra were then analyzed by determining the peak positions.

2.5. Confocal Laser Scanning Microscopy (CLSM)

The method described by Huang et al. [66] was employed with minor modifications to image the microstructures of the chitosan-coated alginate microgels. First, chitosan was dissolved in 200 mL of acetic acid solution (0.1 mol/L) to obtain a 10 mg/mL chitosan solution, and 100 mL of methanol and 10 mL of FITC solution (2.0 mg/mL) were added. Then, the mixed solution was heated in a water bath at 70 °C in the dark with magnetic stirring at 150 rpm for 24 h to stain the chitosan. The microgels were coated with the stained chitosan in the synthesis step. The pH levels of the suspensions were adjusted to 3, 4, 5, 6, and 7 with HCl or NaOH, respectively. A small amount of the diluted microgel suspension was placed on a glass slide, and the coverslip was carefully covered to form a thin sample layer. Then, the slide was held under the microscope. Microstructure images of the microgels were acquired using a model EVO 50XVP confocal laser scanning microscope (Carl Zeiss, CZ Microscopy GmbH, Jena, Germany). Ar/K and He/Ne dual-channel laser mode was used. Fluorescein isothiocyanate (FITC) was excited with a laser at a wavelength of 495 nm. Image acquisition was performed with a $40\times$ and $60\times$ oil lens.

2.6. Dynamic Interfacial Tension and Dilatational Interfacial Rheology

Measurements of the dynamic interfacial tension between the oil and water were performed using a pendant-drop tensiometer (CAM 200, KSV, Biolin Scientific, Stockholm, Sweden). Data were analyzed using drop-shape analysis software (Attension Theta Software, V. 4.1.9.8, Biolin Scientific, Stockholm, Sweden). The Young–Laplace equation was used for curve fitting. Measurements were performed after a pendant drop of the aqueous phase was formed in the oil phase, which was in a quartz cell (Hellma Analytics, Müllheim, Germany). The aqueous phase consisted of a microgel suspension of 1% in ultrapure water. The pH of the aqueous phase was adjusted to 3–7 with NaOH or HCl in each case. The oil phase consisted of washed sunflower oil to remove all interfacially active compounds, which was verified via interfacial tension measurements.

Dilatational interfacial rheology measurements were performed using the piezoelectric PD200 module of the same instrument. The measurements were performed once the interface had reached equilibrium, which was after approximately 10,000 s of adsorption. Harmonic oscillations of deformation amplitude ($\Delta A/A_0 = 5 \pm 1\%$) were applied to the pendant drop with a varying oscillation frequency of 0.01–0.25 Hz. The storage modulus G' and loss modulus G'' were calculated with OscDrop2008 software (Attension Theta Software, V. 4.1.9.8, Biolin Scientific, Stockholm, Sweden). The viscoelastic behavior of the microgel interface was also represented using Lissajous plots of the surface pressure change ($\Delta\pi$) as a function of relative deformation ($\Delta A/A_0$). The temperature used for all experiments was $25.0 \text{ }^\circ\text{C} \pm 1.0 \text{ }^\circ\text{C}$.

2.7. Preparation and Characterization of Microgel-Stabilized Emulsion

2.7.1. Emulsion Preparation

The aqueous microgel suspensions with different pH levels of 3, 4, 5, 6, and 7 were used as the continuous phase. Sunflower oil was added at 5% and the system was homogenized with high-speed shear at 15,000 for 3 min with an IKA T25 Ultra TURRAX Ultra-homogenizer to obtain a chitosan/alginate microgel-stabilized emulsion with a total mass fraction of microgels of 1%.

2.7.2. Characterization of Emulsion Droplet Size

The size distribution of the oil droplets was measured in a similar way as the microgel particles using a Malvern Mastersizer 2000. The continuous phase refractive index was set at 1.33, while the refractive index for the dispersed phase of the oil droplets (sunflower oil) was set at 1.46. An absorbance value of 0.1 was used for the particles. The calculation of droplet size distribution from the angular scattering data was undertaken on the basis of the Mie equations.

2.7.3. Emulsion Microstructure

The emulsion microstructure was observed with CLSM as described above. A small amount of the emulsion was placed on a glass slide and 10 μL of Nile red was added for oil staining. Ar/K and He/Ne dual-channel laser mode was used. Fluorescein isothiocyanate (FITC) and Nile red were excited with a laser at wavelengths of 495 nm and 625, respectively. Image acquisition was performed using a 40 \times and 60 \times oil lens.

2.7.4. Emulsion Stability Analysis

Storage measurement at room temperature ($25.0 \text{ }^\circ\text{C} \pm 1.0 \text{ }^\circ\text{C}$) was employed. Each of the microgel-stabilized emulsions was sealed in a 50 mL falcon plastic tube and stored at $25.0 \text{ }^\circ\text{C} \pm 1.0 \text{ }^\circ\text{C}$. Phase separation of the emulsion samples stored for 1, 3, and 7 days was observed macroscopically. The results of the macroscopical observations were complemented with an analysis of droplet sizes during storage as described above. Each composite microgel-stabilized emulsion sample was prepared at least three times for each measurement.

3. Results

3.1. Particle Characteristics

Figure 1a–e present CLSM images of the microgels at the different pH levels. The microgels formed herein had spherical shapes, as was also found in previous studies [55,66]. As shown in Figure 1f, the freshly prepared microgels presented a core–shell structure (the microscopy image shown in Figure 1f was obtained within 1 h of microgel preparation), whereas, as they aged, the chitosan seemed to be migrating in the interior (the images in Figure 1a–e were taken 1–2 days after microgel preparation).

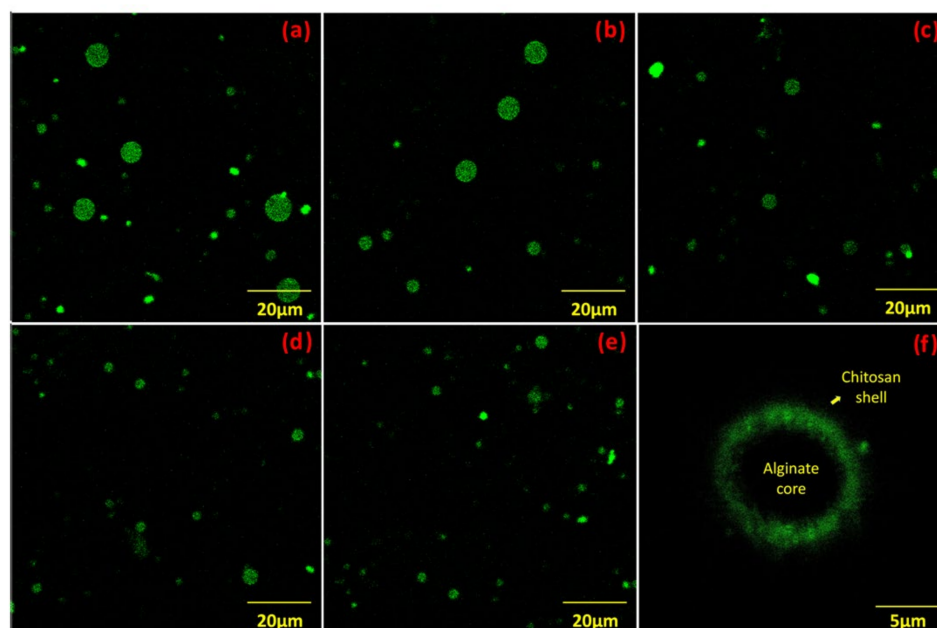


Figure 1. Confocal microscopy images of chitosan-alginate microgels at pH 3 (a), pH 4 (b), pH 5 (c), pH 6 (d), and pH 7 (e). Freshly prepared composite microgel at pH 3 (f).

From the results in Figure 1a–e, it is obvious that there was an effect of pH on the microgel particle size. The effect of pH on particle size can be better observed in Figure 2. The results of both the laser diffraction and CLSM showed that the pH of the particles' dispersion medium had a significant effect on the particle size of the microgels. As the pH decreased, the particle size increased progressively. Furthermore, for the lower pH levels (3, 4, and 5), bimodal particle distribution can be observed in Figure 2, as was also verified via CLSM. Swelling of microgels as a response to changes in the pH of the medium and controlled by the extent of the charging of the particles has long been established [67]. Chitosan adsorbs at the surface of alginate microgels with electrostatic interactions [42,53,64] and, therefore, changes in pH can be expected to affect chitosan adsorption on the interface. Furthermore, the migration of chitosan in the interior of the alginate particles, which was also observed in our work, has been suggested to affect the microgel size via the attraction forces between chitosan and alginate [51]. Microgel aggregation may also take place due to bridging flocculation, since chitosan can adsorb to the surfaces of two or more alginate microgels. Nevertheless, this does not seem to have been the reason for the particle size increase at the lower pH, as verified via CLSM (Figure 1). On the other hand, some interconnection between particles could be observed at pH 7 and, to a lower extent, at pH 6.

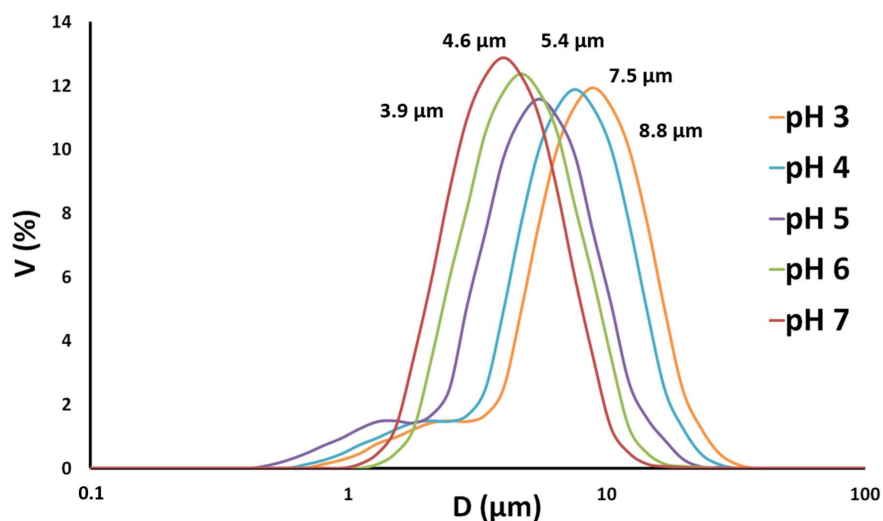


Figure 2. Particle size distribution for chitosan-coated alginate microgels dispersed at different pH levels. D is the particle diameter, and V represents the volume of the respective D within the total particle volume of the suspension.

T_2 relaxation signals obtained by TD-NMR can be analyzed into their components via an inverse Laplace transformation in order to determine the species within the sample that have different mobilities and their respective amounts [68]. Longer relaxation times relate to increased mobility. Figure 3 presents the analysis of the T_2 signal of the microgel dispersions at different pH levels; in addition, the supernatant after centrifugation and a macrogel containing alginate and chitosan were measured.

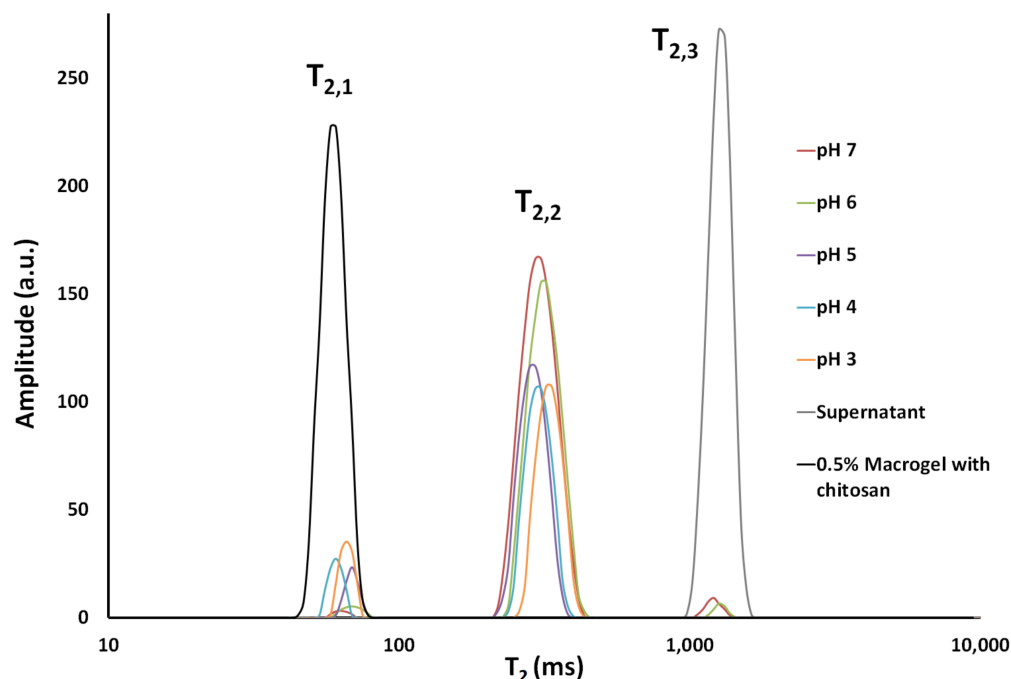


Figure 3. T_2 transverse relaxation signals for microgels at different pH levels and a macrogel analyzed using CONTIN software (version 2DP). $T_{2,1}$, $T_{2,2}$, and $T_{2,3}$ reveal components related to water fractions with different relaxation times.

The spectra of the microgel suspensions presented in Figure 3 reveal the presence of three different water fractions; namely, $T_{2,1}$, $T_{2,2}$, and $T_{2,3}$. The fraction with the largest transverse relaxation time $T_{2,3}$ was assigned to water expelled from the microgel particle

suspension. This was verified by performing the same measurement and analysis with the supernatant after microgel centrifugation. The fact that $T_{2,3}$ was lower than the value for pure water (which is typically 2.4–2.7 s; data not shown) indicated the presence of dissolved macromolecules in this fraction. Secondly, we hypothesized that the two other water fractions could be assigned to the water between the microgel particles ($T_{2,2}$) and the water inside the microgels ($T_{2,1}$). A similar signal interpretation was suggested by Peters et al. [69], who investigated the water-binding capacity of whey protein microparticles. To verify the hypothesis, we centrifuged the microgel dispersions and, instead of using the supernatant, we used the bulk microgels. The results revealed similar transverse relaxation times both for the bulk microgels and the smallest transverse relaxation time. Furthermore, the macrogel presented a similar $T_{2,1}$ value. Regarding the effect of pH on $T_{2,1}$ peak relaxation time, there was no clear tendency that could be determined by our analysis and connect the size of the particles with a more or less swollen structure.

The repartition of amplitudes (and/or areas) between the $T_{2,1}$ and the $T_{2,2}$ peaks reflected the relative amounts of water within and between the microgel particles. It is clear that, for pH 7 and 6, the $T_{2,2}$ peak area was higher, indicating greater amounts of interparticle water. One would expect that repulsion of particles would increase the $T_{2,2}$ peak with respect to the $T_{2,1}$ one. However, in this work, we did not obtain data on the particles' available charges and such an effect could not be assessed. On the other hand, the differences observed in the two water fractions might simply have been due to the fact that the microgel particle suspensions presenting two differently sized populations (as in the case of pH 3, 4, and 5) were packed more densely [70].

3.2. Interfacial Properties

Figure 4 presents the dynamic interfacial tension upon the adsorption of chitosan/alginate microgels at the sunflower oil/water interface at different pH levels. Microgels were present in the suspension at 1%. In addition, measurements of the pure sunflower oil/water system and of the systems containing a solution of alginate and a solution of chitosan were performed for comparison. The interfacial tension for the pure sunflower oil/water system was 27.4 ± 0.1 mN/m, which is typical for culinary oils [71].

The absence of time-dependence for the interfacial tension was due to the removal of surface-active substances prior to the measurement. The interfacial tension of the microgel suspensions in relation to sunflower oil could be grouped into two groups: group (a)—pH 3, 4, and 5; and group (b)—pH 6 and 7. The dynamic process of the adsorption of microgels on the interface was different in the two groups. The microgels at pH 3, 4, and 5 presented a lower rate of decrease for the interfacial tension compared to the microgels at pH 6 and 7. One reason for this behavior could have been the smaller size of the particles in group (b). Equilibrium values for the two groups varied only slightly, with group (a) presenting an equilibrium interfacial tension of 16.6 ± 0.1 mN/m and group (b) 15.9 ± 0.2 mN/m. The value of the equilibrium interfacial tension was closer to that of chitosan rather than alginate, supporting the presence of chitosan hydrophobic groups on the chitosan-alginate particle surface. The values obtained herein were typical for microgel particles adsorbed at oil/water interfaces [1,7,72,73]. The results showed that the chitosan-coated alginate microgels could effectively reduce the oil/water interfacial tension by adsorbing spontaneously onto the interface. Use of more hydrophobic chitosan (higher degree of deacetylation) would be expected to further decrease the water–oil interfacial tension of such particles.

To gain further insight into the properties of the interface, the rheological properties of the interface were investigated under harmonic dilatational perturbations. Interfacial dilatational rheology provides combined information on intra- and intermolecular associations within an interfacial layer. Figure 5 presents the dynamic interfacial rheological parameters G' and G'' (elasticity and viscosity) for the microgel suspension/sunflower oil interface. Measurements were performed once the interface had reached equilibrium as

confirmed by interfacial tension measurements. The interfacial rheological behavior of the chitosan/alginate microgel suspensions was investigated at different pH values. The results showed that G' was generally higher than G'' at all frequencies, indicating that the interface was more elastic than viscous. G' and G'' increased with increasing frequency from 0.01 up to 0.1 Hz, which was expected behavior.

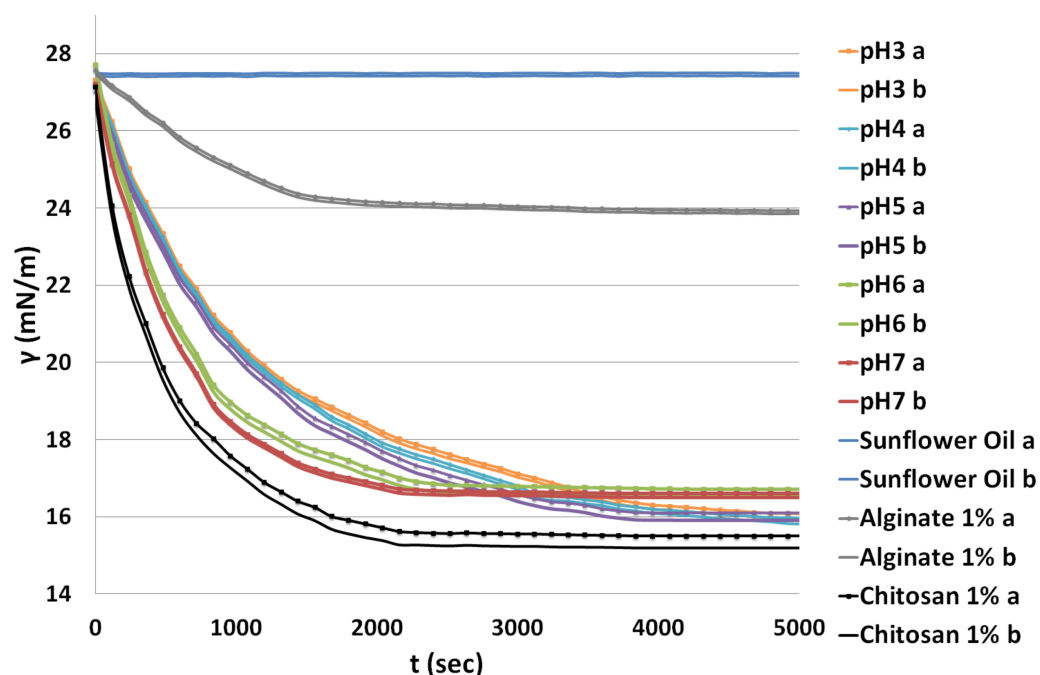


Figure 4. Dynamic interfacial tension (γ) as a function of time (t) at a water/sunflower oil interface. The aqueous solutions contained chitosan-alginate microgels at different pH levels: pure sunflower oil/water system, sunflower oil/alginate solution (pH 7), and sunflower oil/chitosan solution (pH 3). a and b represent two repetitions of the measurement.

The elastic and viscous modulus of the chitosan-alginate microgels was higher than other microgel systems [1,13,66,74] and, given the relatively good adsorption of the particles at the interface (Figure 4), this could lead to good emulsion stability.

The viscoelastic behavior of the microgels was highly dependent on the pH. The elastic modulus (G') was significantly higher for microgels with lower pH values (3, 4, and 5) than for those with higher pH values (6 and 7). Brugger et al. [3] also observed pH dependence for the interfacial viscoelasticity of poly(*N*-isopropylacrylamide)-*co*-methacrylic acid microgels at the water-heptane interface. Given that the adsorption of particles at the interface did not seem to differ significantly (Figure 4), one explanation could be that larger, bimodally distributed particles form a thicker and more densely packed interfacial layer on the interface, as is also true for the bulk (Figure 3). Again, the effect of particle surface charges could not be assessed here but, based on the data provided in the literature, one would expect a decrease in zeta potential from positive to close to zero values at pH 7 [64] and a weakening of the electrostatic interactions, resulting in weaker repulsive forces between the particles and reduced swelling. As the microgels swell, their intrinsic viscoelasticity is affected, which can lead to an increase in the elastic modulus (G') [75]. This is because the swollen microgels are more likely to be subject to rearrangement and restructuring of their network when deformed, resulting in increased resistance to deformation and a higher elastic modulus. Furthermore, at lower pH values, positively charged microgels are expected to adsorb more strongly at negatively charged oil/water interfaces [76], which may also contribute to an increase in the elastic modulus (G'). Nevertheless, this stronger adsorption was not observed in the interfacial tension measurements.

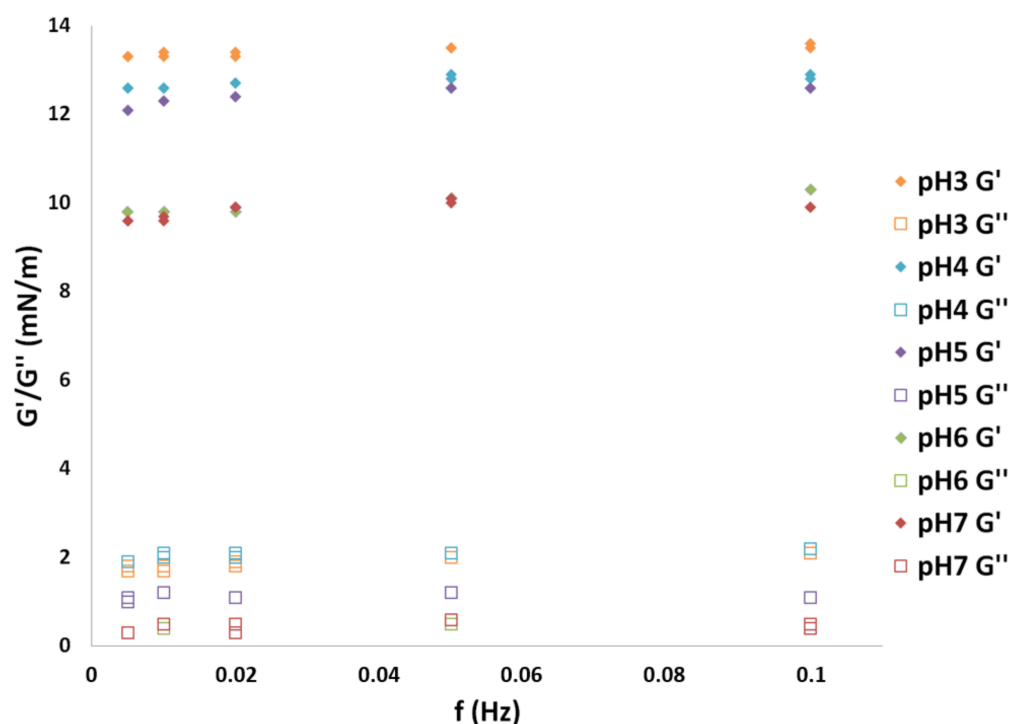


Figure 5. Dynamic dilatational interfacial elasticity (G') and viscosity (G'') for oil/water interfaces with adsorbed chitosan-coated alginate microgels.

The viscoelastic response of the interface can be also observed in the Lissajous plots presented in Figure 6, where the transition from a rather linear elastic rheological response of the interface at lower pH to a more linear viscoelastic one is evident.

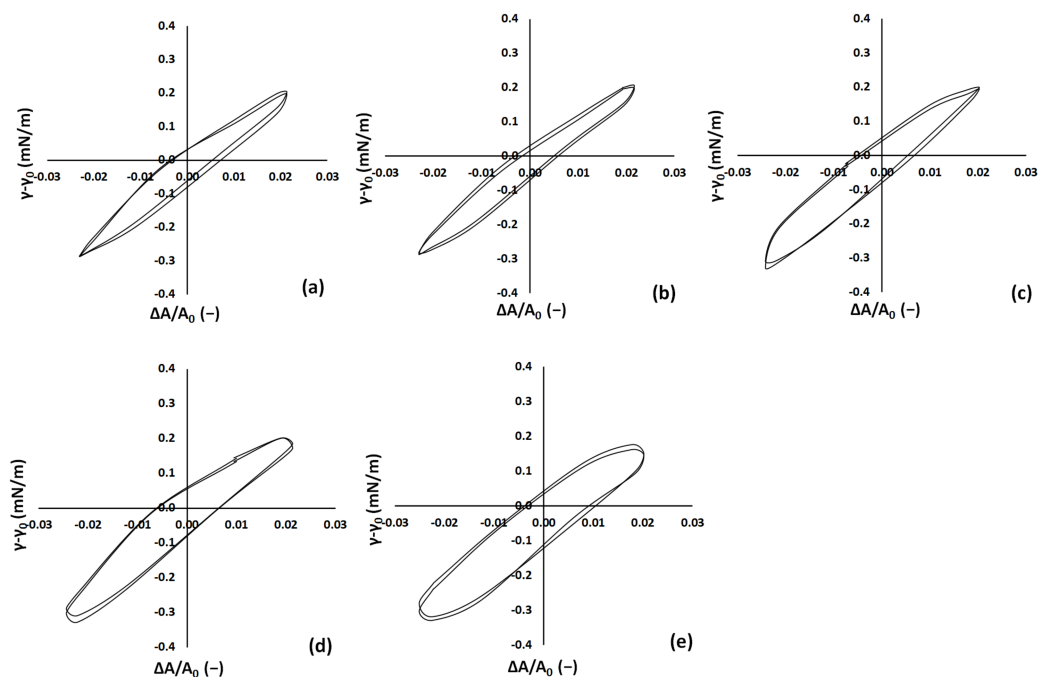


Figure 6. Lissajous plots presenting the rheological behavior of the interfacial layer of the microgels adsorbed at the oil/water interface: (a–e) show the results for pH 3, 4, 5, 6, and 7, respectively.

Overall, the results suggest that the chitosan/alginate microgel suspensions could form a gel-like structure at the interface, with the rigidity of the structure depending on the

pH and particle size. These results have implications for the design of food formulations, where interfacial properties play a critical role in product stability and functionality.

3.3. Emulsion Stability

Figure 7 presents indicative photos of the emulsions stabilized by alginate-chitosan microgels. All emulsions were macroscopically stable (i.e., did not present phase separation) during storage for more than 1 week. In order to gain deeper insights into the performance of the microgel-stabilized emulsions, the droplet sizes of the emulsions were determined using light scattering.

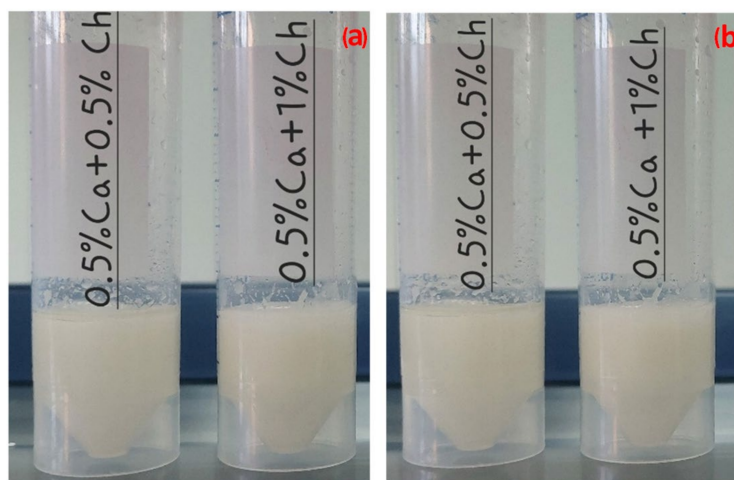


Figure 7. Emulsions stabilized by chitosan-alginate microgels with different concentrations of chitosan at pH 7 (a) right after their formation and (b) after 7 days of storage at 25 °C.

Figure 8 presents the volume-average droplet diameter $D[4,3]$ for the emulsions right after their formation and during storage for 1 week. Emulsions at pH 3, 4, 5, 6, and 7, as well as with concentrations of microgel suspension of 1% and 5%, were prepared. It was obvious that the emulsion characteristics at the time of formation (0 days in Figure 8) as expressed by the droplet sizes, as well as their stability (as depicted by the evolution of droplet sizes during storage), were significantly affected by the microgel suspension properties. Smaller droplet sizes were achieved at pH values of 3, 4, and 5 that changed only a little—and, at pH 4, non-significantly—during storage, demonstrating the high stability of the formed systems. On the other hand, larger droplet sizes were observed at pH 6 and even larger ones at pH 7. Moreover, at pH 6 and 7, high rates of droplet size increase were observed, although the emulsions did not show any signs of macroscopic destabilization during the period of observation (Figure 7). Given the observed droplet size increase at pH 6 and 7, these emulsions were expected to destabilize in a few weeks.

In order to gain further insight into the behavior of the emulsions stabilized by the microgels at different pH levels, CLSM analysis of the emulsions was applied at pH 4 (stable emulsion with unchanging droplet sizes) and pH 7 (macroscopically stable emulsion for 1 week with significant changes in particle sizes during the same period) (Figure 9). At pH 7, we could observe cases of bridging between droplets, whereas droplets appeared as separate at pH 4. Therefore, bridging flocculation seems to be a plausible mechanism explaining the destabilization at the higher pH levels where particle charges were also expected to be lower. Regarding the effect of the concentration of microgel particles in the suspension (1% or 5%) on emulsion stability, there was no such effect at pH 3, 4, or 5.

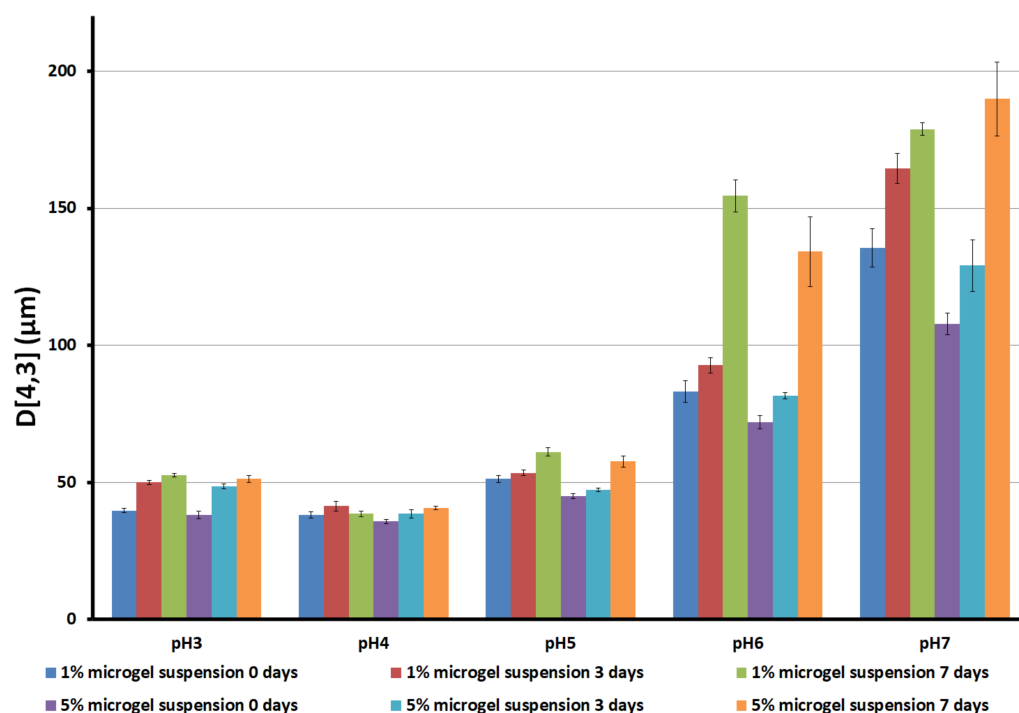


Figure 8. Volume-average mean droplet size $D[4,3]$ for the microgel particle-stabilized sunflower-oil-in-water emulsions stored for up to 7 days as a function of the pH of the microgel suspension.

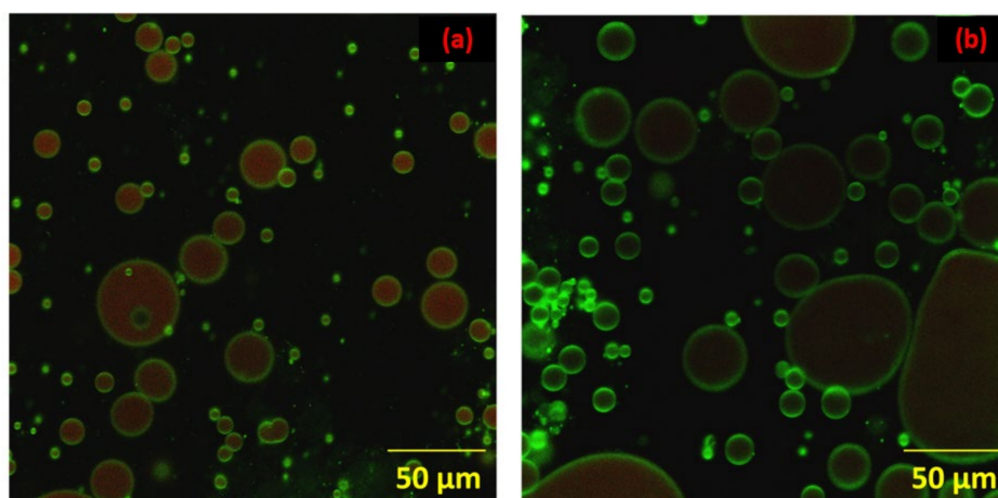


Figure 9. Confocal microscopy images of emulsions at pH 4 (a) and pH 7 (b).

The behavior changed at pH 6 and 7. At these higher pH values, increasing the concentration of microgel particles initially induced a decrease in droplet sizes, possibly due to the fast coverage of the interface with the microgel particles in the emulsions with more concentrated particles. However, the rate of the droplet size increase was higher at higher concentrations, and this was in line with the bridging flocculation interpretation.

4. Conclusions

In this work, chitosan-coated alginate microgels were prepared at different pH levels, characterized, and further used as emulsifiers. The microgels were prepared using the top-down approach. Coating of the alginate particles with chitosan resulted in the initial formation of a core-shell structure with the chitosan particles situated at the periphery of the spherical particles. Within one to two days, this core-shell structure had vanished and

chitosan penetrated the interior of the particle, as evidenced via CLSM, therefore indicating the rearrangement of the chitosan-alginate molecules within the particle. The microgel particles were adsorbed at the water–oil interface and the water–oil interfacial tension was typical for such systems [1]. Microgel adsorption at the water–oil interface indicated the presence of the hydrophobic chitosan groups on the particles' surface. The degree of deacetylation of the chitosan used herein was 90%. If the degree of deacetylation were increased—and, therefore, the hydrophobicity of the chitosan—this could lead to a decrease in water–oil interfacial tension and, therefore, stronger adsorption at the interface.

The pH was a decisive variable affecting the microgel particle characteristics. The increase in pH from 3 to 7 resulted in a significant decrease in microgel particle size, with pH levels of 3, 4, and 5 presenting bimodal particle size distributions. TD-NMR measurements were performed in order to assess the potential swelling behavior of the microgel particles as a function of pH. No persistent trend was observed for the T_2 relaxation time assigned to the water within the particles. Therefore, in our study, it was not clear whether the effect of pH on microgel particle sizes was due to the formation of more swollen structures that could not be determined via TD-NMR or the different performance of the gel during high-shear breakage and the formation of the microgels. To the best of the authors' knowledge, this is the first time that TD-NMR has been applied to investigate swelling in such systems, and further investigation is required in the future in order to assess the information that can be obtained for microgels by using this method. Another result was that TD-NMR indicated different packing of microgel particles in the aqueous phase (due to different quantities of interparticle water) as a function of pH. This could be attributed, at least in part, to the higher packing of bimodal particle distributions compared to monomodal ones. Microgels at different pH levels presented similar equilibrium interfacial tension; however, the rate of the decrease in interfacial tension was pH-dependent and at least partly particle size-dependent. The effect of particle charge was not examined in the present work; however, based on the work by Nan et al. [64], a decrease in alginate-chitosan microgel particle charge can be expected as pH increases. The dynamic interfacial viscoelasticity measurements showed high viscoelasticity for the interfacial layer, with G' close to 14 mN/m at a frequency of 0.1 Hz. The viscoelastic behavior transitioned from a purely linear elastic regime at the lower pH values investigated here to a more viscoelastic one at pH 7. The thicker interfacial layer of the larger particles and the better packing of the bimodal distribution at lower pH values were related to this behavior.

The sunflower-oil-in-water emulsions formed using the microgels as emulsifier were volumetrically stable for 1 week, and no separation of water, oil, or oil droplet flocks could be observed at any of the pH levels (3–7) or microgel particle concentrations (1%, 5%) examined. However, laser diffraction showed a particle size increase attributed to bridging flocculation when the results of the laser diffraction were compared with the CLSM.

The systems prepared herein presented increased emulsification stability compared to previous work [64]. It is possible that the formation of a thick, highly viscoelastic interfacial layer for the charged particles provided good emulsion stability. The systems prepared herein could be a promising solution for the preparation of low-fat mayonnaises and dressings without the use of other emulsifiers or expensive emulsification methods. High shear was enough as an energy input for emulsion formation. Emulsions were highly stable at acidic pH, which is the pH range of these foods (the pH of mayonnaise is 4). The effect of pH on the stability of the emulsions could have potential applications involving the release of bioactive compounds in the digestive system.

Author Contributions: Conceptualization, E.P.K.; methodology, E.P.K. and A.C.; formal analysis, E.P.K. and A.C.; investigation, A.C.; writing—original draft preparation, E.P.K. and A.C.; writing—review and editing, E.P.K.; supervision, E.P.K.; funding acquisition, E.P.K. All authors have read and agreed to the published version of the manuscript.

Funding: This work was funded by the Oils and Interfaces (OLIE) group www.oilsinterfaces.eu (accessed on 15 January 2023).

Data Availability Statement: Data available upon reasonable request to the corresponding author.

Acknowledgments: The good collaboration between the members of the OLIE group is acknowledged by the authors. All members of the OLIE group have consented to the acknowledgement.

Conflicts of Interest: The authors declare no conflict of interest.

References

1. Brugger, B.; Richtering, W. Emulsions Stabilized by Stimuli-Sensitive Poly(N-Isopropylacrylamide)-Co-Methacrylic Acid Polymers: Microgels versus Low Molecular Weight Polymers. *Langmuir* **2008**, *24*, 7769–7777. [[CrossRef](#)]
2. Dickinson, E. Microgels—An Alternative Colloidal Ingredient for Stabilization of Food Emulsions. *Trends Food Sci. Technol.* **2015**, *43*, 178–188. [[CrossRef](#)]
3. Lyon, L.A.; Fernandez-Nieves, A. The Polymer/Colloid Duality of Microgel Suspensions. *Annu. Rev. Phys. Chem.* **2012**, *63*, 25–43. [[CrossRef](#)] [[PubMed](#)]
4. Ngai, T.; Auweter, H.; Behrens, S.H. Environmental Responsiveness of Microgel Particles and Particle-Stabilized Emulsions. *Macromolecules* **2006**, *39*, 8171–8177. [[CrossRef](#)]
5. Liang, J.; Teng, F.; Chou, T.M.; Libera, M. Measuring Microgel Swell Ratio by Cryo-SEM. *Polymer* **2017**, *116*, 1–4. [[CrossRef](#)]
6. Schmidt, S.; Liu, T.; Rütten, S.; Phan, K.H.; Möller, M.; Richtering, W. Influence of Microgel Architecture and Oil Polarity on Stabilization of Emulsions by Stimuli-Sensitive Core-Shell Poly(N-Isopropylacrylamide-Co-Methacrylic Acid) Microgels: Mickering versus Pickering Behavior? *Langmuir* **2011**, *27*, 9801–9806. [[CrossRef](#)]
7. Wu, Y.; Wiese, S.; Balaceanu, A.; Richtering, W.; Pich, A. Behavior of Temperature-Responsive Copolymer Microgels at the Oil/Water Interface. *Langmuir* **2014**, *30*, 7660–7669. [[CrossRef](#)]
8. Ishii, T.; Matsumiya, K.; Aoshima, M.; Matsumura, Y. Microgelation Imparts Emulsifying Ability to Surface-Inactive Polysaccharides—Bottom-up vs Top-down Approaches. *NPJ Sci. Food* **2018**, *2*, 15. [[CrossRef](#)]
9. Hu, M.; Wu, Y.; Wang, J.; Lu, W.; Gao, Z.; Xu, L.; Cui, S.; Fang, Y.; Nishinari, K. Emulsions Stabilization and Lipid Digestion Profiles of Sodium Alginate Microgels: Effect of the Crosslink Density. *Food Biophys.* **2021**, *16*, 346–354. [[CrossRef](#)]
10. Rayner, M. Current Status on Novel Ways for Stabilizing Food Dispersions by Oleosins, Particles and Microgels. *Curr. Opin. Food Sci.* **2015**, *3*, 94–109. [[CrossRef](#)]
11. Kwok, M.H.; Sun, G.; Ngai, T. Microgel Particles at Interfaces: Phenomena, Principles, and Opportunities in Food Sciences. *Langmuir* **2019**, *35*, 4205–4217. [[CrossRef](#)]
12. Kwok, M.H.; Ngai, T. A Confocal Microscopy Study of Micron-Sized Poly(N-Isopropylacrylamide) Microgel Particles at the Oil-Water Interface and Anisotropic Flattening of Highly Swollen Microgel. *J. Colloid Interface Sci.* **2016**, *461*, 409–418. [[CrossRef](#)]
13. Brugger, B.; Vermant, J.; Richtering, W. Interfacial Layers of Stimuli-Responsive Poly-(N-Isopropylacrylamide-Co-Methacrylic acid) (PNIPAM-Co-MAA) Microgels Characterized by Interfacial Rheology and Compression Isotherms. *Phys. Chem. Chem. Phys.* **2010**, *12*, 14573–14578. [[CrossRef](#)]
14. Destribats, M.; Lapeyre, V.; Sellier, E.; Leal-Calderon, F.; Schmitt, V.; Ravaine, V. Water-in-Oil Emulsions Stabilized by Water-Dispersible Poly(N-Isopropylacrylamide) Microgels: Understanding Anti-Finkle Behavior. *Langmuir* **2011**, *27*, 14096–14107. [[CrossRef](#)]
15. Dickinson, E. Biopolymer-Based Particles as Stabilizing Agents for Emulsions and Foams. *Food Hydrocoll.* **2017**, *68*, 219–231. [[CrossRef](#)]
16. Torres, O.; Murray, B.; Sarkar, A. Emulsion Microgel Particles: Novel Encapsulation Strategy for Lipophilic Molecules. *Trends Food Sci. Technol.* **2016**, *55*, 98–108. [[CrossRef](#)]
17. Qian, C.; Decker, E.A.; Xiao, H.; McClements, D.J. Physical and Chemical Stability of β -Carotene-Enriched Nanoemulsions: Influence of PH, Ionic Strength, Temperature, and Emulsifier Type. *Food Chem.* **2012**, *132*, 1221–1229. [[CrossRef](#)]
18. Destribats, M.; Eyharts, M.; Lapeyre, V.; Sellier, E.; Varga, I.; Ravaine, V.; Schmitt, V. Impact of PNIPAM Microgel Size on Its Ability to Stabilize Pickering Emulsions. *Langmuir* **2014**, *30*, 1768–1777. [[CrossRef](#)]
19. De Freitas, R.A.; Nicolai, T.; Chassenieux, C.; Benyahia, L. Stabilization of Water-in-Water Emulsions by Polysaccharide-Coated Protein Particles. *Langmuir* **2016**, *32*, 1227–1232. [[CrossRef](#)]
20. Paques, J.P.; Van Der Linden, E.; Van Rijn, C.J.M.; Sagis, L.M.C. Preparation Methods of Alginate Nanoparticles. *Adv. Colloid Interface Sci.* **2014**, *209*, 163–171. [[CrossRef](#)]
21. Pravinata, L.; Akhtar, M.; Bentley, P.J.; Mahatnirunkul, T.; Murray, B.S. Preparation of Alginate Microgels in a Simple One Step Process via the Leeds Jet Homogenizer. *Food Hydrocoll.* **2016**, *61*, 77–84. [[CrossRef](#)]
22. Burey, P.; Bhandari, B.R.; Howes, T.; Gidley, M.J. Hydrocolloid Gel Particles: Formation, Characterization, and Application. *Crit. Rev. Food Sci. Nutr.* **2008**, *48*, 361–377. [[CrossRef](#)] [[PubMed](#)]
23. Farjami, T.; Madadlou, A. Fabrication Methods of Biopolymeric Microgels and Microgel-Based Hydrogels. *Food Hydrocoll.* **2017**, *62*, 262–272. [[CrossRef](#)]
24. Joye, I.J.; McClements, D.J. Biopolymer-Based Nanoparticles and Microparticles: Fabrication, Characterization, and Application. *Curr. Opin. Colloid Interface Sci.* **2014**, *19*, 417–427. [[CrossRef](#)]
25. Murray, B.S. Microgels at Fluid-Fluid Interfaces for Food and Drinks. *Adv. Colloid Interface Sci.* **2019**, *271*, 101990. [[CrossRef](#)]

26. Shewan, H.M.; Stokes, J.R. Review of Techniques to Manufacture Micro-Hydrogel Particles for the Food Industry and Their Applications. *J. Food Eng.* **2013**, *119*, 781–792. [[CrossRef](#)]
27. Bassani, A.; Montes, S.; Jubete, E.; Palenzuela, J.; Sanjuán, A.P.; Spigno, G. Incorporation of Waste Orange Peels Extracts into PLA Films. *Chem. Eng. Trans.* **2019**, *74*, 1063–1068. [[CrossRef](#)]
28. Kavanagh, G.M.; Ross-Murphy, S.B. Rheological characterisation of polymer gels. *Prog. Polym. Sci.* **1998**, *23*, 533–562. [[CrossRef](#)]
29. Saavedra Isusi, G.I.; Karbstein, H.P.; van der Schaaf, U.S. Microgel Particle Formation: Influence of Mechanical Properties of Pectin-Based Gels on Microgel Particle Size Distribution. *Food Hydrocoll.* **2019**, *94*, 105–113. [[CrossRef](#)]
30. Guo, J.; Zhou, Q.; Liu, Y.C.; Yang, X.Q.; Wang, J.M.; Yin, S.W.; Qi, J.R. Preparation of Soy Protein-Based Microgel Particles Using a Hydrogel Homogenizing Strategy and Their Interfacial Properties. *Food Hydrocoll.* **2016**, *58*, 324–334. [[CrossRef](#)]
31. Jiao, B.; Shi, A.; Wang, Q.; Binks, B.P. High-Internal-Phase Pickering Emulsions Stabilized Solely by Peanut-Protein-Isolate Microgel Particles with Multiple Potential Applications. *Angew. Chem. Int. Ed.* **2018**, *57*, 9274–9278. [[CrossRef](#)]
32. Matsumiya, K.; Murray, B.S. Soybean Protein Isolate Gel Particles as Foaming and Emulsifying Agents. *Food Hydrocoll.* **2016**, *60*, 206–215. [[CrossRef](#)]
33. Sarkar, A.; Murray, B.; Holmes, M.; Ettelaie, R.; Abdalla, A.; Yang, X. In Vitro Digestion of Pickering Emulsions Stabilized by Soft Whey Protein Microgel Particles: Influence of Thermal Treatment. *Soft Matter* **2016**, *12*, 3558–3569. [[CrossRef](#)]
34. Zhang, S.; Holmes, M.; Ettelaie, R.; Sarkar, A. Pea Protein Microgel Particles as Pickering Stabilisers of Oil-in-Water Emulsions: Responsiveness to PH and Ionic Strength. *Food Hydrocoll.* **2020**, *102*, 105583. [[CrossRef](#)]
35. Mumper, R.J.; Hoffman, A.S.; Puolakkainen, P.A.; Bouchard, L.S.; Gombotz, W.R. Calcium-Alginate Beads for the Oral Delivery of Transforming Growth Factor- β 1 (TGF- β 1): Stabilization of TGF- β 1 by the Addition of Polyacrylic Acid within Acid-Treated Beads. *J. Control. Release* **1994**, *30*, 241–251. [[CrossRef](#)]
36. Segi, N.; Yotsuyanagi, T.; Ikeda, K. Interaction of Calcium-Induced Alginate Gel Beads with Propranolol. *Chem. Pharm. Bull.* **1989**, *37*, 3092–3095. [[CrossRef](#)]
37. Rinaudo, M. Chitin and Chitosan: Properties and Applications. *Prog. Polym. Sci.* **2006**, *31*, 603–632. [[CrossRef](#)]
38. Klinkesorn, U. The Role of Chitosan in Emulsion Formation and Stabilization. *Food Rev. Int.* **2013**, *29*, 371–393. [[CrossRef](#)]
39. Li, X.; Xia, W. Effects of Concentration, Degree of Deacetylation and Molecular Weight on Emulsifying Properties of Chitosan. *Int. J. Biol. Macromol.* **2011**, *48*, 768–772. [[CrossRef](#)]
40. Payet, L.; Terentjev, E.M. Emulsification and Stabilization Mechanisms of O/W Emulsions in the Presence of Chitosan. *Langmuir* **2008**, *24*, 12247–12252. [[CrossRef](#)]
41. Nilsen-Nygaard, J.; Strand, S.P.; Vårum, K.M.; Draget, K.I.; Nordgård, C.T. Chitosan: Gels and Interfacial Properties. *Polymers* **2015**, *7*, 552–579. [[CrossRef](#)]
42. Gåserød, O.; Jolliffe, I.G.; Hampson, F.C.; Dettmar, P.W.; Skjak-Bræk, G. The Enhancement of the Bioadhesive Properties of Calcium Alginate Gel Beads by Coating with Chitosan. *Int. J. Pharm.* **1998**, *175*, 237–246. [[CrossRef](#)]
43. Imeson, A. (Ed.) *Food Stabilisers, Thickeners, and Gelling Agents*; Blackwell Pub: Oxford, UK, 2010; ISBN 9781405132671. [[CrossRef](#)]
44. Gombotz, W.R.; Fong Wee, S. Protein Release from Alginate Matrices. *Adv. Drug Deliv. Rev.* **1998**, *31*, 267–285. [[CrossRef](#)] [[PubMed](#)]
45. Krasaekoopt, W.; Bhandari, B.; Deeth, H. The Influence of Coating Materials on Some Properties of Alginate Beads and Survivability of Microencapsulated Probiotic Bacteria. *Int. Dairy J.* **2004**, *14*, 737–743. [[CrossRef](#)]
46. Alexakis, T.; Boadu, D.K.; Quong, D.; Groboillot, A.; O’neill, I.; Poncet, D.; Neufeld, R.J. Microencapsulation of DNA Within Alginate Microspheres and Crosslinked Chitosan Membranes for In Vivo Application. *Appl. Biochem. Biotechnol.* **1995**, *50*, 93–106. [[CrossRef](#)]
47. Ribeiro, A.J.; Neufeld, R.J.; Arnaud, P.; Chaumeil, J.C. Microencapsulation of Lipophilic Drugs in Chitosan-Coated Alginate Microspheres. *Int. J. Pharm.* **1999**, *187*, 115–123. [[CrossRef](#)]
48. Taqieddin, E.; Amiji, M. Enzyme Immobilization in Novel Alginate-Chitosan Core-Shell Microcapsules. *Biomaterials* **2004**, *25*, 1937–1945. [[CrossRef](#)]
49. Ribeiro, A.J.; Silva, C.; Ferreira, D.; Veiga, F. Chitosan-Reinforced Alginate Microspheres Obtained through the Emulsification/Internal Gelation Technique. *Eur. J. Pharm. Sci.* **2005**, *25*, 31–40. [[CrossRef](#)]
50. You, J.O.; Liu, Y.C.; Peng, C.A. Efficient Gene Transfection Using Chitosan-Alginate Core-Shell Nanoparticles. *Int. J. Nanomed.* **2006**, *1*, 173–180. [[CrossRef](#)]
51. Zhang, Y.; Wei, W.; Lv, P.; Wang, L.; Ma, G. Preparation and Evaluation of Alginate-Chitosan Microspheres for Oral Delivery of Insulin. *Eur. J. Pharm. Biopharm.* **2011**, *77*, 11–19. [[CrossRef](#)]
52. Conti, B.; Colzani, B.; Papetti, A.; Mascherpa, D.; Dorati, R.; Genta, I.; Pruzzo, C.; Signoretto, C.; Zaura, E.; Lingström, P.; et al. Adhesive Microbeads for the Targeting Delivery of Anticaries Agents of Vegetable Origin. *Food Chem.* **2013**, *138*, 898–904. [[CrossRef](#)]
53. Feng, R.; Wang, L.; Zhou, P.; Luo, Z.; Li, X.; Gao, L. Development of the PH Responsive Chitosan-Alginate Based Microgel for Encapsulation of Juglans Regia L. Polyphenols under Simulated Gastrointestinal Digestion in Vitro. *Carbohydr. Polym.* **2020**, *250*, 116917. [[CrossRef](#)]
54. Seth, A.; Lafargue, D.; Poirier, C.; Péan, J.M.; Ménager, C. Performance of Magnetic Chitosan-Alginate Core-Shell Beads for Increasing the Bioavailability of a Low Permeable Drug. *Eur. J. Pharm. Biopharm.* **2014**, *88*, 374–381. [[CrossRef](#)]

55. Qin, C.; Zhou, J.; Zhang, Z.; Chen, W.; Hu, Q.; Wang, Y. Convenient One-Step Approach Based on Stimuli-Responsive Sol-Gel Transition Properties to Directly Build Chitosan-Alginate Core-Shell Beads. *Food Hydrocoll.* **2019**, *87*, 253–259. [[CrossRef](#)]
56. Dickinson, E. Flocculation of Protein-Stabilized Oil-in-Water Emulsions. *Colloids Surf. B* **2010**, *81*, 130–140. [[CrossRef](#)]
57. Chevalier, Y.; Bolzinger, M.A. Emulsions Stabilized with Solid Nanoparticles: Pickering Emulsions. *Colloids Surf. A Physicochem. Eng. Asp.* **2013**, *439*, 23–34. [[CrossRef](#)]
58. Berton-Carabin, C.C.; Schroën, K. Pickering Emulsions for Food Applications: Background, Trends, and Challenges. *Annu. Rev. Food Sci. Technol.* **2015**, *6*, 263–297. [[CrossRef](#)]
59. Richtering, W. Responsive Emulsions Stabilized by Stimuli-Sensitive Microgels: Emulsions with Special Non-Pickering Properties. *Langmuir* **2012**, *28*, 17218–17229. [[CrossRef](#)]
60. Zhou, G.; Lu, Y.; Zhang, H.; Chen, Y.; Yu, Y.; Gao, J.; Sun, D.; Zhang, G.; Zou, H.; Zhong, Y. A Novel Pulsed Drug-Delivery System: Polyelectrolyte Layer-by-Layer Coating of Chitosan-Alginate Microgels. *Int. J. Nanomed.* **2013**, *8*, 877–887. [[CrossRef](#)]
61. Duffy, C.; O’Sullivan, M.; Jacquier, J.C. Preparation of Novel Chitosan Iron Microgel Beads for Fortification Applications. *Food Hydrocoll.* **2018**, *84*, 608–615. [[CrossRef](#)]
62. Yeung, T.W.; Üçok, E.F.; Tiani, K.A.; McClements, D.J.; Sela, D.A. Microencapsulation in Alginate and Chitosan Microgels to Enhance Viability of Bifidobacterium Longum for Oral Delivery. *Front. Microbiol.* **2016**, *7*, 494. [[CrossRef](#)] [[PubMed](#)]
63. Matricardi, P.; Di Meo, C.; Coviello, T.; Alhaique, F. Recent Advances and Perspectives on Coated Alginate Microspheres for Modified Drug Delivery. *Expert Opin. Drug Deliv.* **2008**, *5*, 417–425. [[CrossRef](#)] [[PubMed](#)]
64. Nan, F.; Wu, J.; Qi, F.; Liu, Y.; Ngai, T.; Ma, G. Uniform Chitosan-Coated Alginate Particles as Emulsifiers for Preparation of Stable Pickering Emulsions with Stimulus Dependence. *Colloids Surf. A Physicochem. Eng. Asp.* **2014**, *456*, 246–252. [[CrossRef](#)]
65. Provencher, S.W. A constrained regularization method for inverting data represented by linear algebraic or integral equations. *Comput. Phys. Commun.* **1982**, *27*, 213–227. [[CrossRef](#)]
66. Huang, M.; Khor, E.; Lim, L.Y. Uptake and Cytotoxicity of Chitosan Molecules and Nanoparticles: Effects of Molecular Weight and Degree of Deacetylation. *Pharm. Res.* **2004**, *21*, 344–353. [[CrossRef](#)]
67. Fernández-Nieves, A.; Fernández-Barbero, A.; Vincent, B.; De Las Nieves, F.J. Charge Controlled Swelling of Microgel Particles. *Macromolecules* **2000**, *33*, 2114–2118. [[CrossRef](#)]
68. Forshult, S.E. Quantitative Analysis with Pulsed NMR and the CONTIN Computer Program. 2004. Available online: <http://urn.kb.se/resolve?urn=urn:nbn:se:kau:diva-2588> (accessed on 20 December 2022).
69. Peters, J.P.C.M.; Vergeldt, F.J.; Van As, H.; Luyten, H.; Boom, R.M.; van der Goot, A.J. Time Domain Nuclear Magnetic Resonance as a Method to Determine and Characterize the Water-Binding Capacity of Whey Protein Microparticles. *Food Hydrocoll.* **2016**, *54*, 170–178. [[CrossRef](#)]
70. Averardi, A.; Cola, C.; Zeltmann, S.E.; Gupta, N. Effect of Particle Size Distribution on the Packing of Powder Beds: A Critical Discussion Relevant to Additive Manufacturing. *Mater. Today* **2020**, *24*, 100964. [[CrossRef](#)]
71. Dopierala, K.; Javadi, A.; Krägel, J.; Schano, K.H.; Kalogianni, E.P.; Leser, M.E.; Miller, R. Dynamic Interfacial Tensions of Dietary Oils. *Colloids Surf. A Physicochem. Eng. Asp.* **2011**, *382*, 261–265. [[CrossRef](#)]
72. Li, Z.; Richtering, W.; Ngai, T. Poly(N-Isopropylacrylamide) Microgels at the Oil-Water Interface: Temperature Effect. *Soft Matter* **2014**, *10*, 6182–6191. [[CrossRef](#)]
73. Monteux, C.; Marlière, C.; Paris, P.; Pantoustier, N.; Sanson, N.; Perrin, P. Poly(N-Isopropylacrylamide) Microgels at the Oil-Water Interface: Interfacial Properties as a Function of Temperature. *Langmuir* **2010**, *26*, 13839–13846. [[CrossRef](#)]
74. Deshmukh, O.S.; Van Den Ende, D.; Stuart, M.C.; Mugele, F.; Duits, M.H.G. Hard and Soft Colloids at Fluid Interfaces: Adsorption, Interactions, Assembly & Rheology. *Adv. Colloid Interface Sci.* **2015**, *222*, 215–227. [[CrossRef](#)]
75. Fernandez-Rodriguez, M.A.; Martín-Molina, A.; Maldonado-Valderrama, J. Microgels at Interfaces, from Micking Emulsions to Flat Interfaces and Back. *Adv. Colloid Interface Sci.* **2021**, *288*, 102350. [[CrossRef](#)]
76. Marinova, K.G.; Alargova, R.G.; Denkov, N.D.; Veleev, O.D.; Petsev, D.N.; Ivanov, I.B.; Borwankar, R.P. Charging of Oil-Water Interfaces Due to Spontaneous Adsorption of Hydroxyl Ions. *Langmuir* **1996**, *12*, 2045–2051. [[CrossRef](#)]

Disclaimer/Publisher’s Note: The statements, opinions and data contained in all publications are solely those of the individual author(s) and contributor(s) and not of MDPI and/or the editor(s). MDPI and/or the editor(s) disclaim responsibility for any injury to people or property resulting from any ideas, methods, instructions or products referred to in the content.